Interval Arithmetic-Based Approach to Tolerance Analysis of Monopulse Linear Antenna Arrays

N. Anselmi, P. Rocca, and A. Massa

2024/12/13

Contents

1 Commons Vulnerability Analysis

GOAL: TO UNDERSTAND THE MOST CRITICAL ELEMENTS AMONG THE COMMONS ELEMENTS OF A RECONFIGURABLE ARRAY.

- Performances are analyzed in terms of SLL and BW for both the services (Σ and Δ patterns).
- We are considering an increasing number of commons elements: $P = 2, 4, 6, 8$.
- **Maximum widths** intervals are used, that is, considering normalized amplitudes, the n-th faulty common element's interval amplitude is equal to $\mathbf{A}_n = [0.0,\ 1.0]$

Cases of study:

- $F = 1$: Single faulty element among the P commons elements.
- $F = 2$: Double faulty element among the P commons elements.

1.1 PERFORMANCES and WORST CASES in terms of SLL - $F = 1$:

Performances:

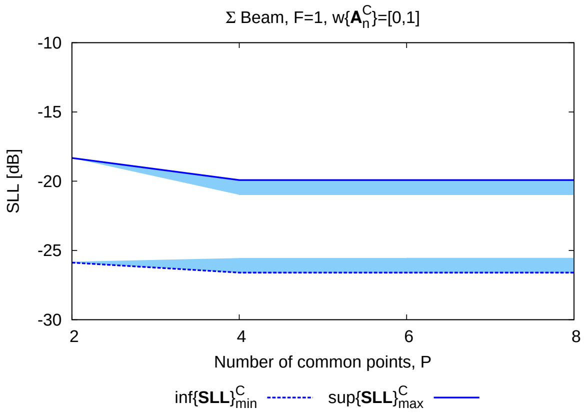

Figure 2. Sum Pattern **SLL** vs P

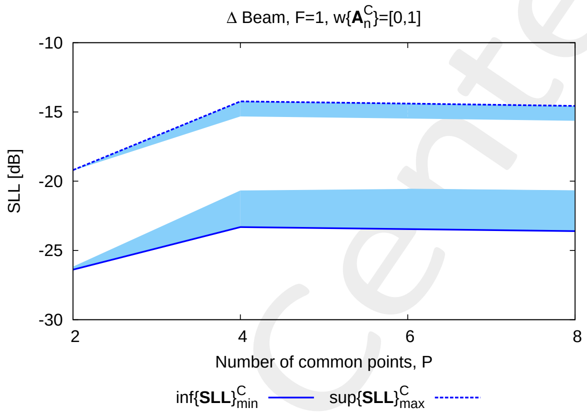

Figure 3. Difference Pattern **SLL** vs P

P	$\inf\{\mathbf{SLL}\}^C_{min}$	$\inf\{\mathbf{SLL}\}^C_{max}$	$\sup\{\mathbf{SLL}\}^C_{min}$	$\sup\{\mathbf{SLL}\}^C_{max}$
2	-25.88	-25.81	-18.33	-18.33
4	-26.6	-25.56	-20.98	-19.92
6	-26.6	-25.56	-20.98	-19.92
8	-26.6	-25.56	-20.98	-19.92

Table 1. Sum Pattern **SLL** values

P	$\inf\{\mathbf{SLL}\}^C_{min}$	$\inf\{\mathbf{SLL}\}^C_{max}$	$\sup\{\mathbf{SLL}\}^C_{min}$	$\sup\{\mathbf{SLL}\}^C_{max}$
2	-26.39	-26.17	-19.23	-19.20
4	-23.31	-20.67	-15.32	-14.24
6	-23.46	-20.56	-15.47	-14.39
8	-23.60	-20.68	-15.64	-14.56

Table 2. Difference Pattern **SLL** values

Worst Cases - SLL analysis - $F = 1$:

In the following the patterns and excitations of the worst cases in terms of $\sup\{\mathbf{SLL}\}_{max}^{C}$ are reported.

- $P = 2$

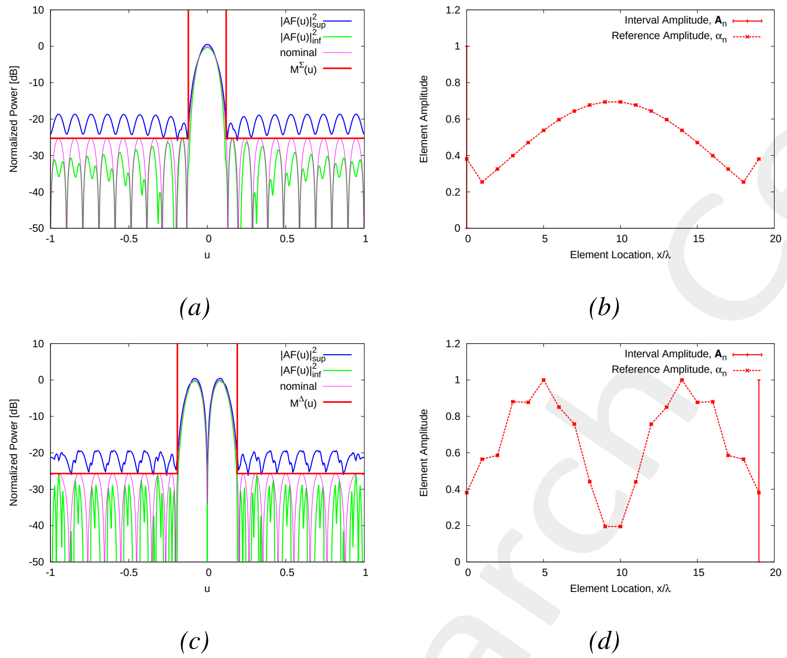

Figure 4. Radiation patterns *(a)(c)* and amplitudes *(b)(d)* for the worst sum beam *(a)(b)* and difference beam *(c)(d)* in terms of SLL, considering $F = 1$.

- $P = 4$

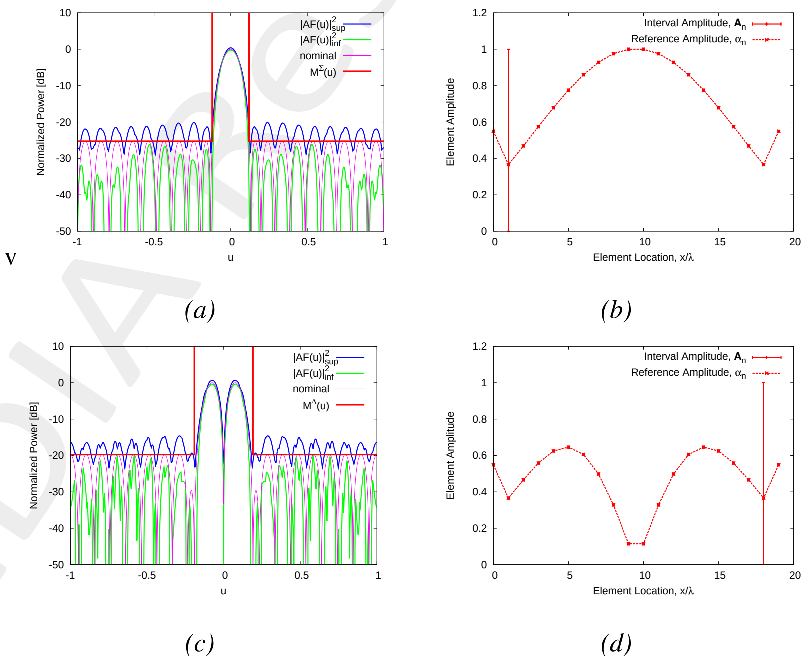

Figure 5. Radiation patterns *(a)(c)* and amplitudes *(b)(d)* for the worst sum beam *(a)(b)* and difference beam *(c)(d)* in terms of SLL, considering $F = 1$.

- $P = 6$

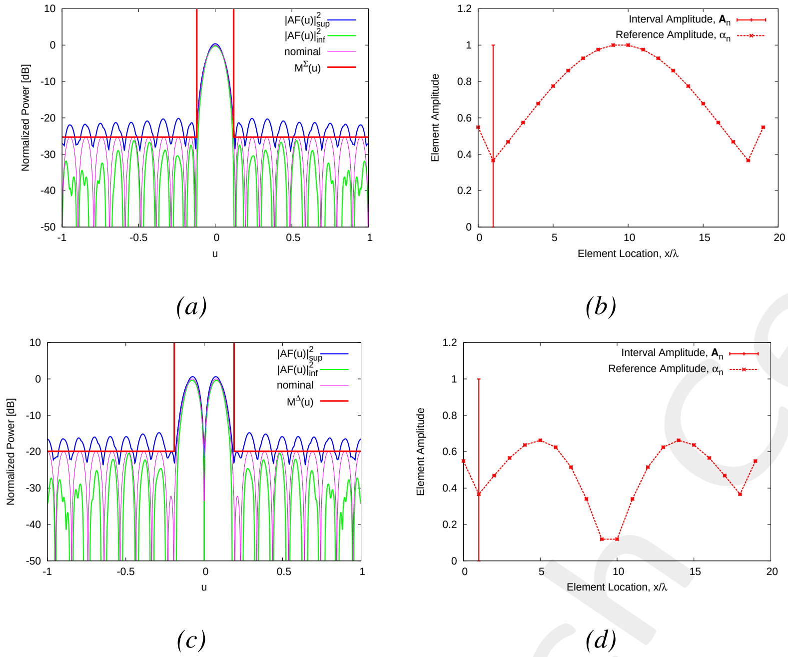

Figure 6. Radiation patterns *(a)(c)* and amplitudes *(b)(d)* for the worst sum beam *(a)(b)* and difference beam *(c)(d)* in terms of SLL considering $F = 1$.

- $P = 8$

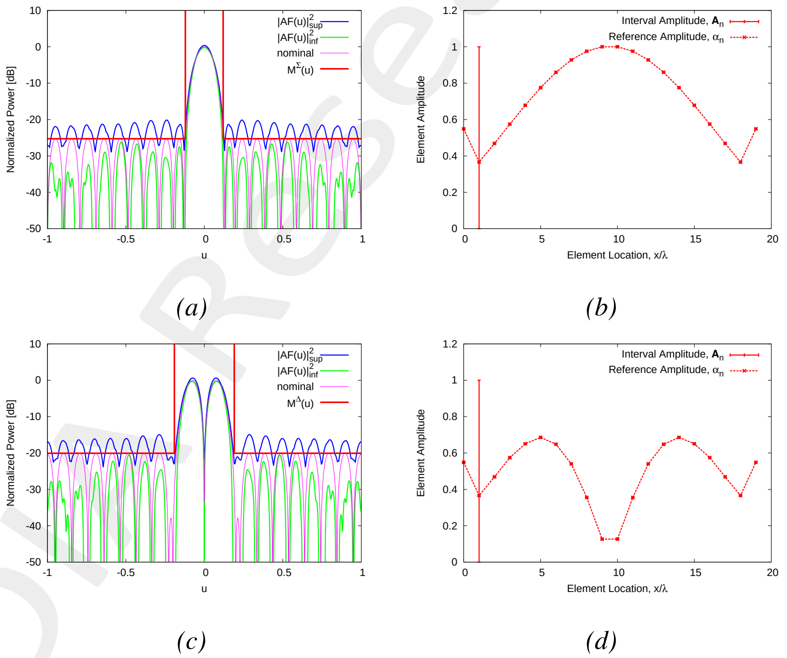

Figure 7. Radiation patterns *(a)(c)* and amplitudes *(b)(d)* for the worst sum beam *(a)(b)* and difference beam *(c)(d)* in terms of SLL, considering $F = 1$.

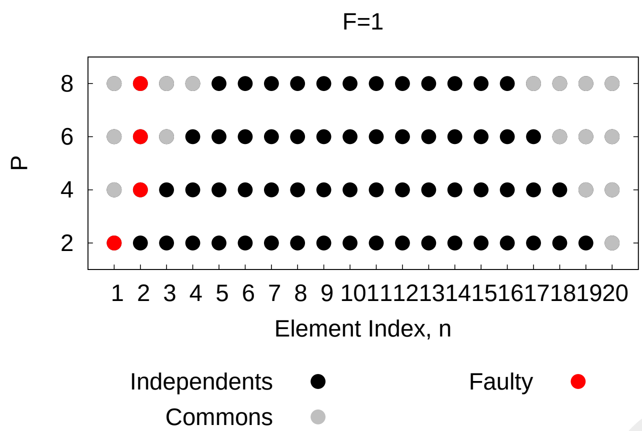

Figure 8. Worst case configurations in terms of SLL computed over the Σ beam, and $F = 1$.

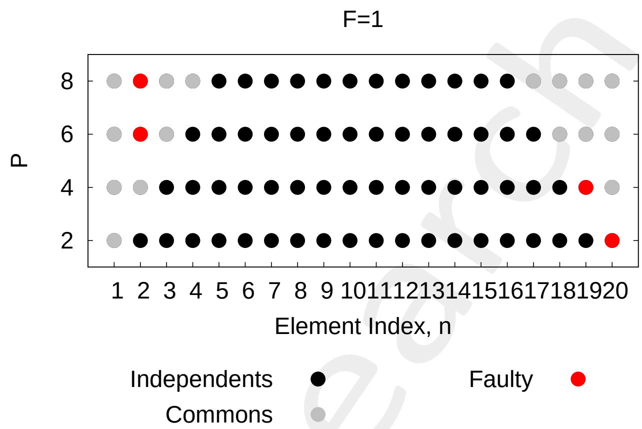

Figure 9. Worst case configurations in terms of SLL computed over the Δ beam, and $F = 1$.

1.2 PERFORMACES and WORST CASES in terms of SLL - $F = 2$:

Performances:

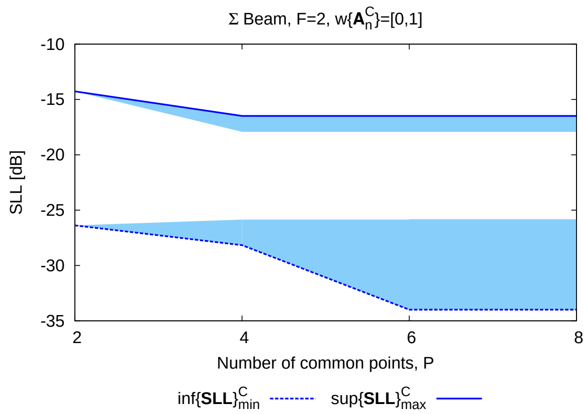

Figure 10. Sum Pattern **SLL** vs P

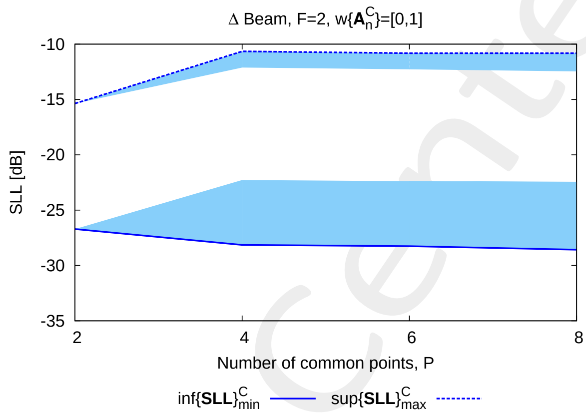

Figure 11. Difference Pattern **SLL** vs P

P	$\inf\{\mathbf{SLL}\}^C_{min}$	$\inf\{\mathbf{SLL}\}^C_{max}$	$\sup\{\mathbf{SLL}\}^C_{min}$	$\sup\{\mathbf{SLL}\}^C_{max}$
2	-26.37	-26.37	-14.26	-14.26
4	-28.16	-25.85	-17.92	-16.49
6	-33.99	-25.85	-17.92	-16.49
8	-33.99	-25.85	-17.92	-16.49

Table 3. Sum Pattern **SLL** values

P	$\inf\{\mathbf{SLL}\}^C_{min}$	$\inf\{\mathbf{SLL}\}^C_{max}$	$\sup\{\mathbf{SLL}\}^C_{min}$	$\sup\{\mathbf{SLL}\}^C_{max}$
2	-26.71	-26.71	-15.37	-15.37
4	-28.14	-22.27	-12.11	-10.65
6	-28.26	-22.38	-12.27	-10.82
8	-28.58	-22.46	-12.46	-10.82

Table 4. Difference Pattern **SLL** values

Worst Cases - SLL analysis - $F = 2$:

In the following the patterns and excitations of the worst cases in terms of $\sup\{\mathbf{SLL}\}^{C}_{max}$ are reported.

- $P = 2$

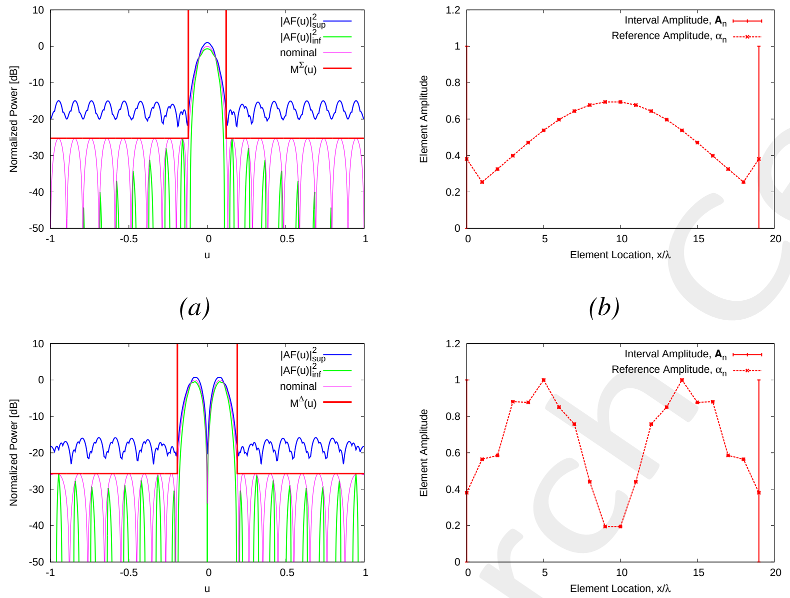

(a) *(b)*

(c) *(d)*

Figure 12. Radiation patterns *(a)(c)* and amplitudes *(b)(d)* for the worst sum beam *(a)(b)* and difference beam *(c)(d)* in terms of SLL, considering $F = 2$.

- $P = 4$

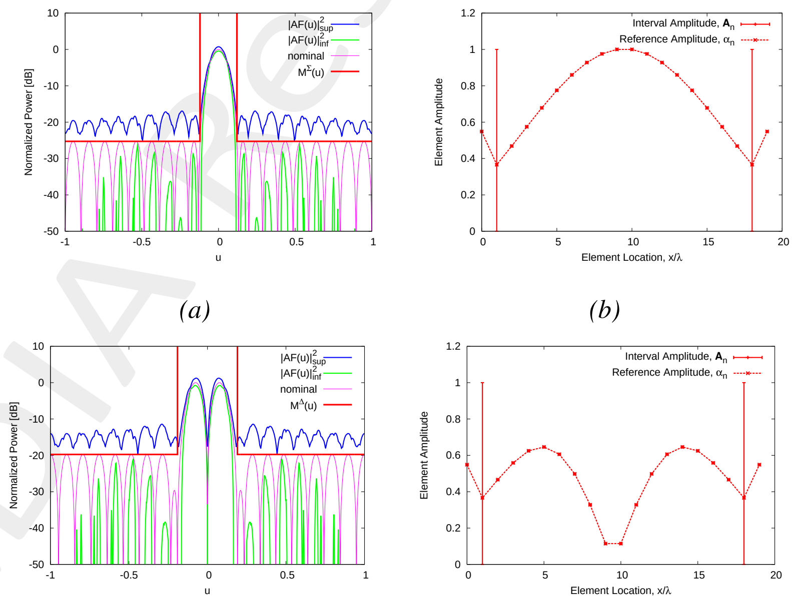

(a) *(b)*

(c) *(d)*

Figure 13. Radiation patterns *(a)(c)* and amplitudes *(b)(d)* for the worst sum beam *(a)(b)* and difference beam *(c)(d)* in terms of SLL, considering $F = 2$.

- $P = 6$

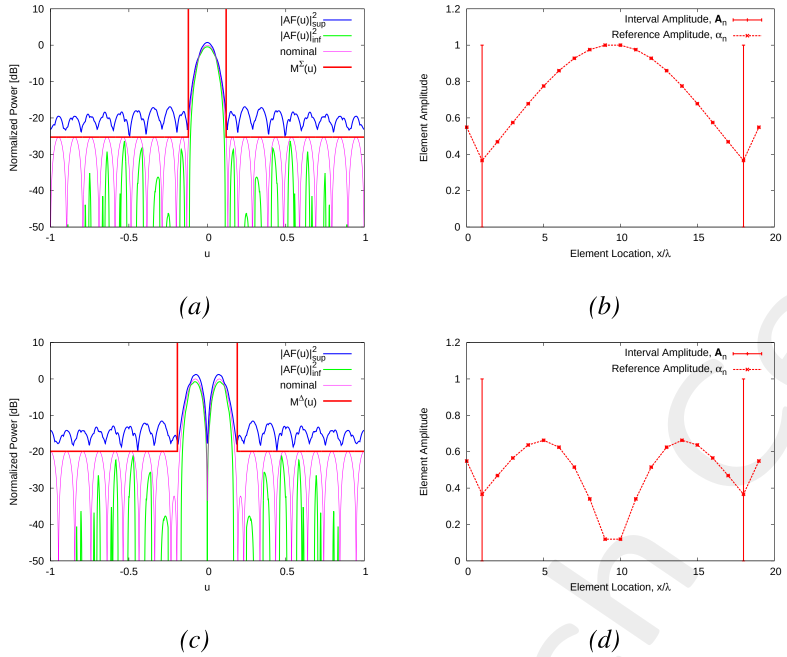

Figure 14. Radiation patterns *(a)(c)* and amplitudes *(b)(d)* for the worst sum beam *(a)(b)* and difference beam *(c)(d)* in terms of SLL, considering $F = 2$.

- $P = 8$

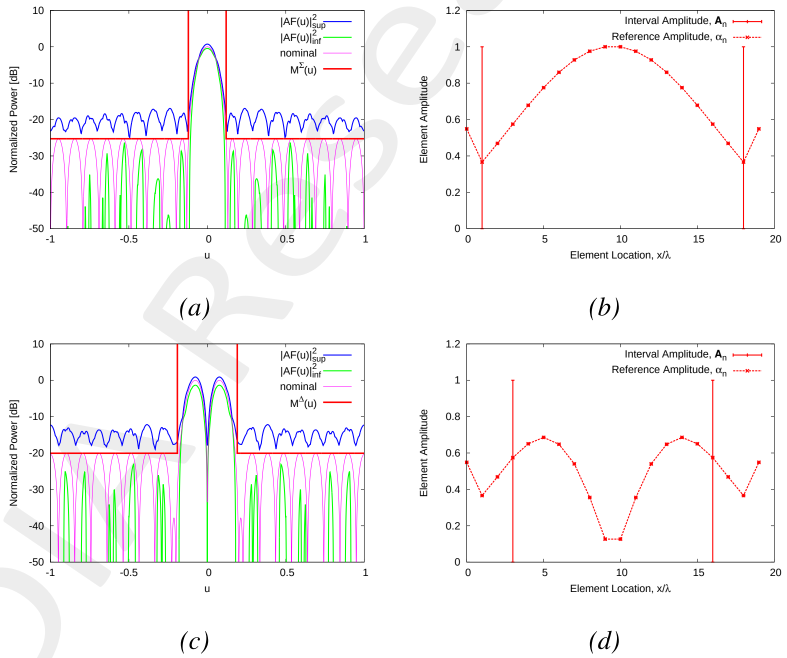

Figure 15. Radiation patterns *(a)(c)* and amplitudes *(b)(d)* for the worst sum beam *(a)(b)* and difference beam *(c)(d)* in terms of SLL, considering $F = 2$.

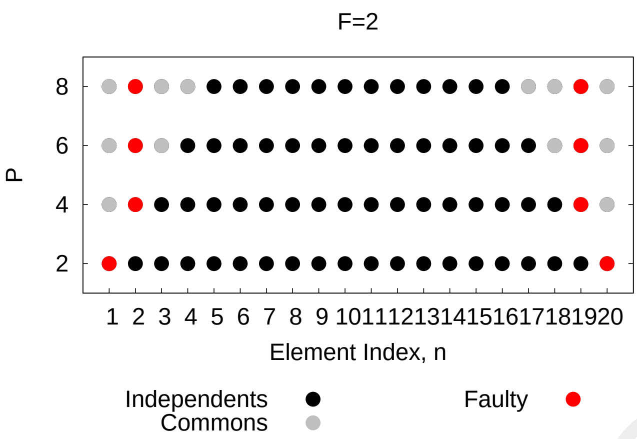

Figure 16. Worst case configurations in terms of SLL computed over the Σ beam, and $F = 2$.

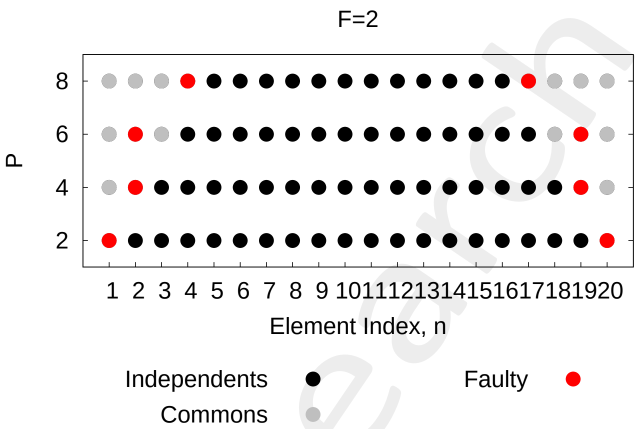

Figure 17. Worst case configurations in terms of SLL computed over the Δ beam, and $F = 2$.

Comments on the results:

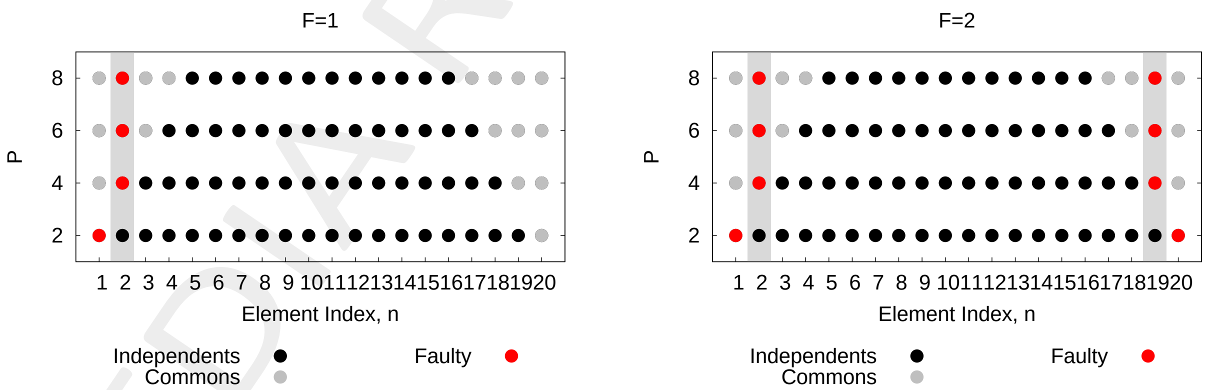

(a) *(b)*

Figure 18. Worst case configurations in terms of SLL performances over the Σ beam considering (a) $F = 1$ and (b) $F = 2$. The shaded gray areas hilights the most critical positions.

As shown by Fig. 18 from the above analysis the most critical elements among the commons, turns out to be the elements with index $n \in \{2, 19\}$. It is worth noting here that these elements correspond to the ones with the minimum amplitude value.

1.3 PERFORMANCES and WORST CASES in terms of BW - $F = 1$:

Performances:

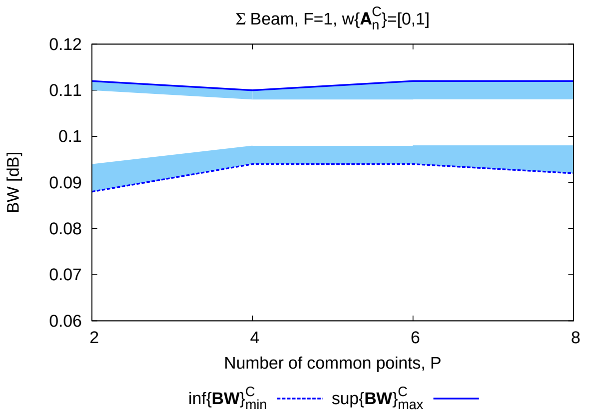

Figure 19. Sum Pattern $\mathbf{BW}$ vs P

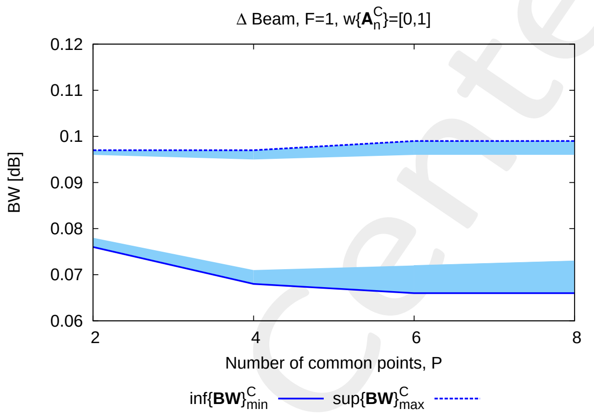

Figure 20. Difference Pattern $\mathbf{BW}$ vs P

P	$\inf\{\mathbf{BW}\}_{min}^C$	$\inf\{\mathbf{BW}\}_{max}^C$	$\sup\{\mathbf{BW}\}_{min}^C$	$\sup\{\mathbf{BW}\}_{max}^C$
2	0.088	0.094	0.110	0.112
4	0.094	0.098	0.108	0.110
6	0.094	0.098	0.108	0.112
8	0.092	0.098	0.108	0.112

Table 5. Sum Pattern $\mathbf{BW}$ values

P	$\inf\{\mathbf{BW}\}_{min}^C$	$\inf\{\mathbf{BW}\}_{max}^C$	$\sup\{\mathbf{BW}\}_{min}^C$	$\sup\{\mathbf{BW}\}_{max}^C$
2	0.076	0.078	0.096	0.097
4	0.068	0.071	0.095	0.097
6	0.066	0.072	0.096	0.099
8	0.066	0.073	0.096	0.099

Table 6. Difference Pattern $\mathbf{BW}$ values

Worst Cases - BW analysis - $F = 1$:

In the following the patterns and excitations of the worst cases in terms of $\sup\{\mathbf{BW}\}^C_{max}$ are reported.

- $P = 2$

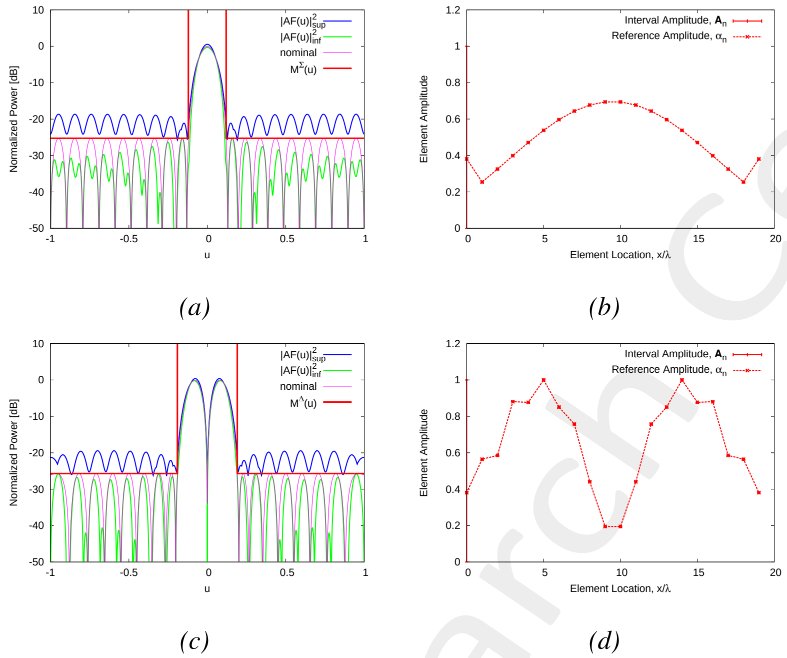

(a) *(b)*

(c) *(d)*

Figure 21. Radiation patterns *(a)(c)* and amplitudes *(b)(d)* for the worst sum beam *(a)(b)* and difference beam *(c)(d)* in terms of BW, considering $F = 1$.

- $P = 4$

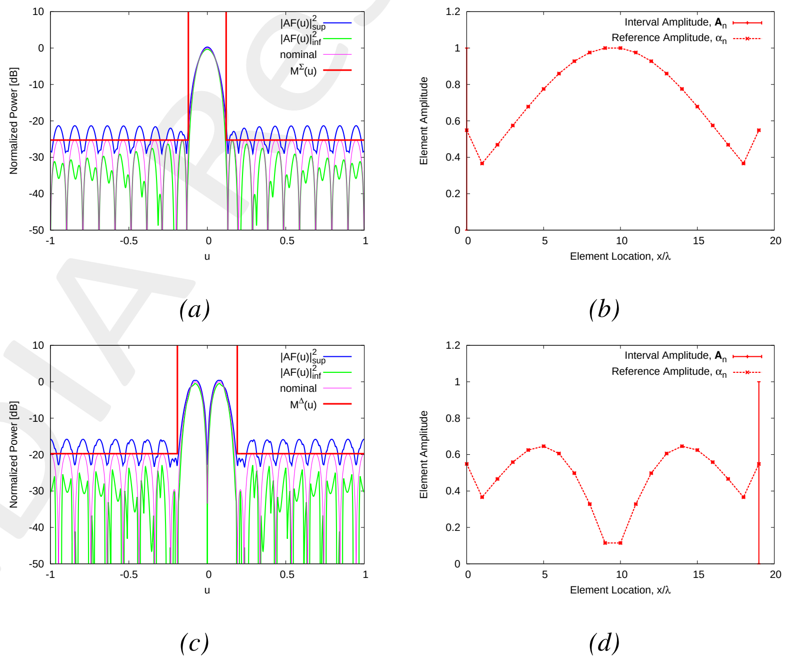

(a) *(b)*

(c) *(d)*

Figure 22. Radiation patterns *(a)(c)* and amplitudes *(b)(d)* for the worst sum beam *(a)(b)* and difference beam *(c)(d)* in terms of BW, considering $F = 1$.

- $P = 6$

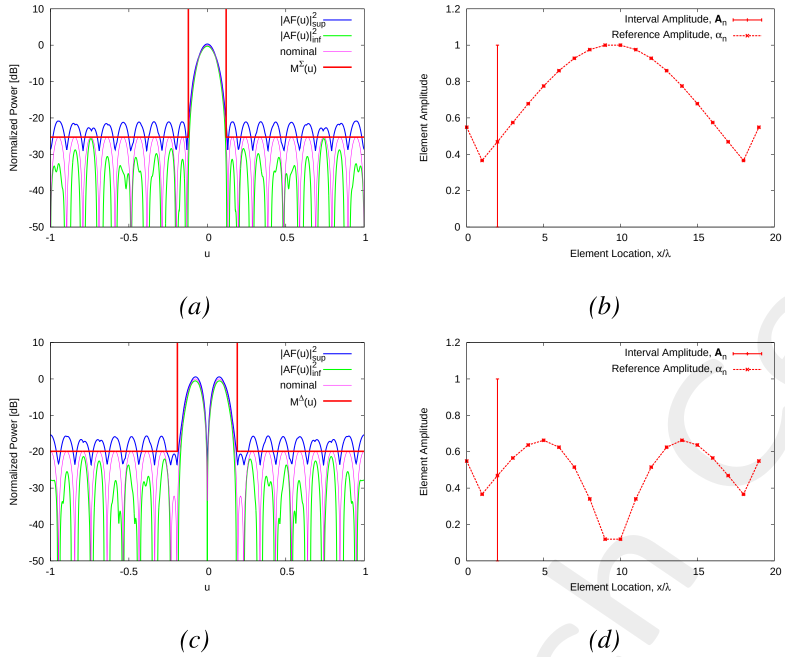

Figure 23. Radiation patterns *(a)(c)* and amplitudes *(b)(d)* for the worst sum beam *(a)(b)* and difference beam *(c)(d)* in terms of BW, considering $F = 1$.

- $P = 8$

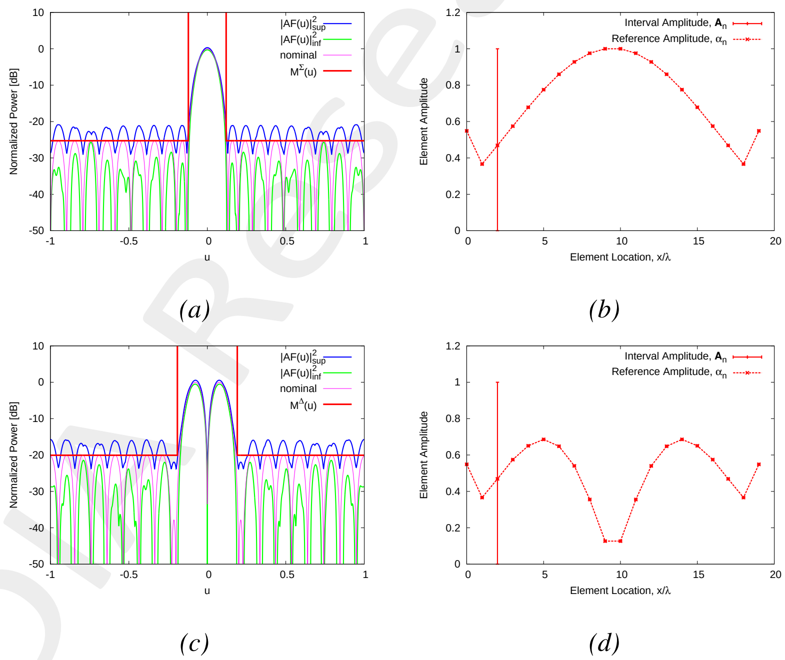

Figure 24. Radiation patterns *(a)(c)* and amplitudes *(b)(d)* for the worst sum beam *(a)(b)* and difference beam *(c)(d)* in terms of BW, considering $F = 1$.

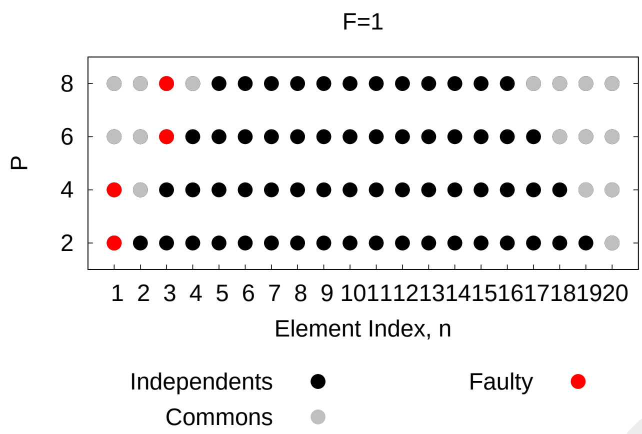

Figure 25. Worst case configurations in terms of BW computed on the Σ beam, and $F = 1$.

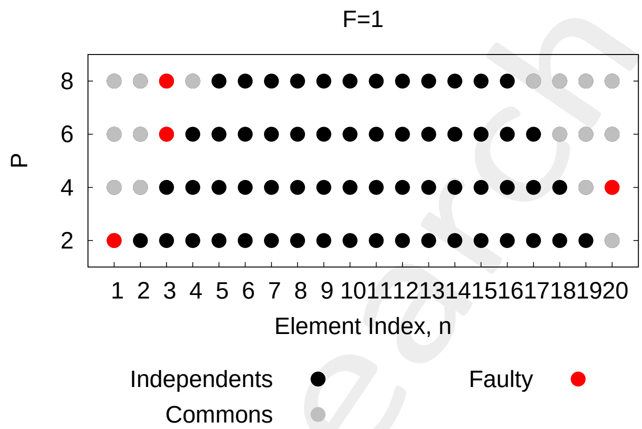

Figure 26. Worst case configurations in terms of BW computed on the Δ beam, and $F = 2$.

1.4 PERFORMANCES and WORST CASES in terms of BW - $F = 2$:

Performances:

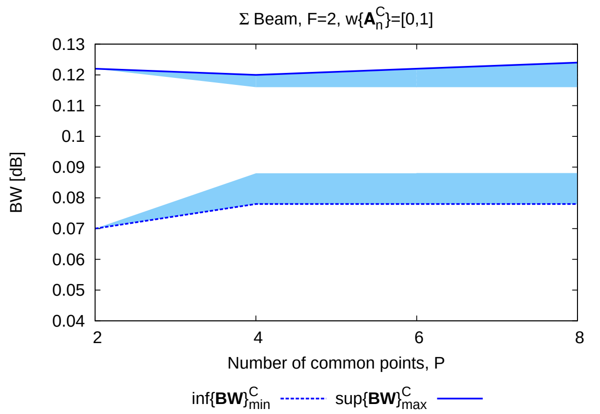

Figure 27. Sum Pattern $\mathbf{BW}$ vs P

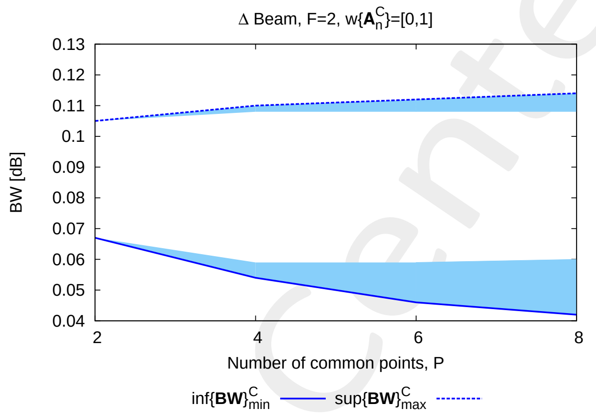

Figure 28. Difference Pattern $\mathbf{BW}$ vs P

P	$\inf\{\mathbf{BW}\}_{min}^C$	$\inf\{\mathbf{BW}\}_{max}^C$	$\sup\{\mathbf{BW}\}_{min}^C$	$\sup\{\mathbf{BW}\}_{max}^C$
2	0.070	0.070	0.122	0.122
4	0.078	0.088	0.116	0.120
6	0.078	0.088	0.116	0.122
8	0.078	0.088	0.116	0.124

Table 7. Sum Pattern $\mathbf{BW}$ values

P	$\inf\{\mathbf{BW}\}_{min}^C$	$\inf\{\mathbf{BW}\}_{max}^C$	$\sup\{\mathbf{BW}\}_{min}^C$	$\sup\{\mathbf{BW}\}_{max}^C$
2	0.067	0.067	0.105	0.105
4	0.054	0.059	0.108	0.110
6	0.046	0.059	0.108	0.112
8	0.042	0.060	0.108	0.114

Table 8. Difference Pattern $\mathbf{BW}$ values

Worst Cases - BW analysis - $F = 2$:

In the following the patterns and excitations of the worst cases in terms of $\sup\{\mathbf{BW}\}^C_{max}$ are reported.

- $P = 2$

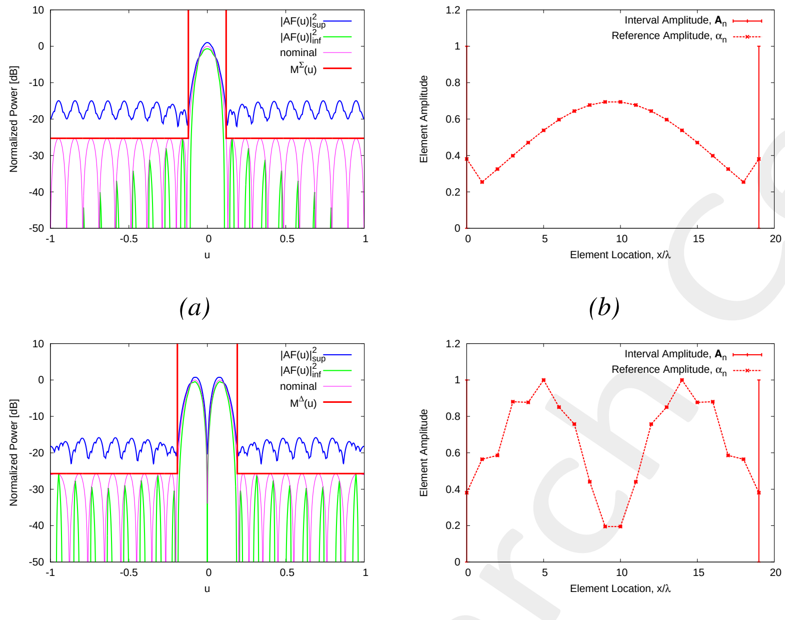

(c) (d)

Figure 29. Radiation patterns *(a)(c)* and amplitudes *(b)(d)* for the worst sum beam *(a)(b)* and difference beam *(c)(d)* in terms of BW, considering $F = 2$.

- $P = 4$

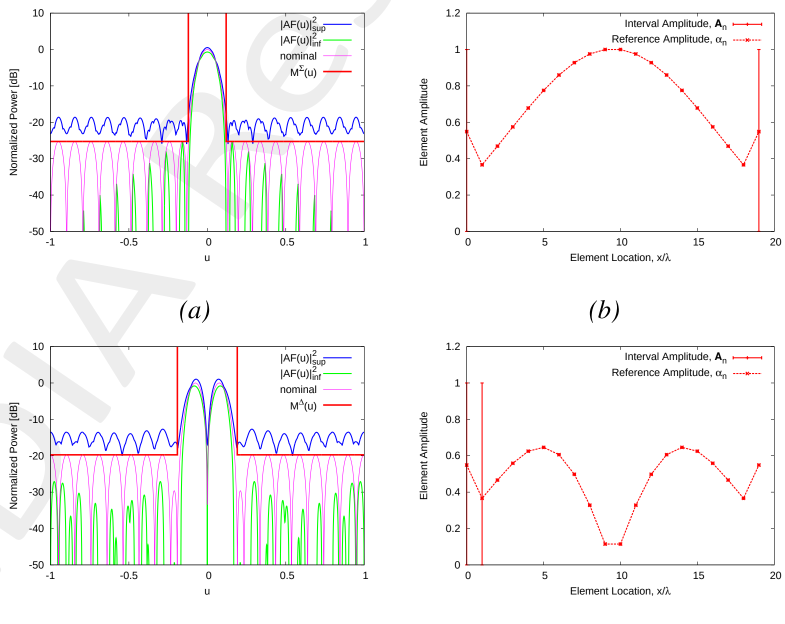

(c) (d)

Figure 30. Radiation patterns *(a)(c)* and amplitudes *(b)(d)* for the worst sum beam *(a)(b)* and difference beam *(c)(d)* in terms of BW, considering $F = 2$.

- $P = 6$

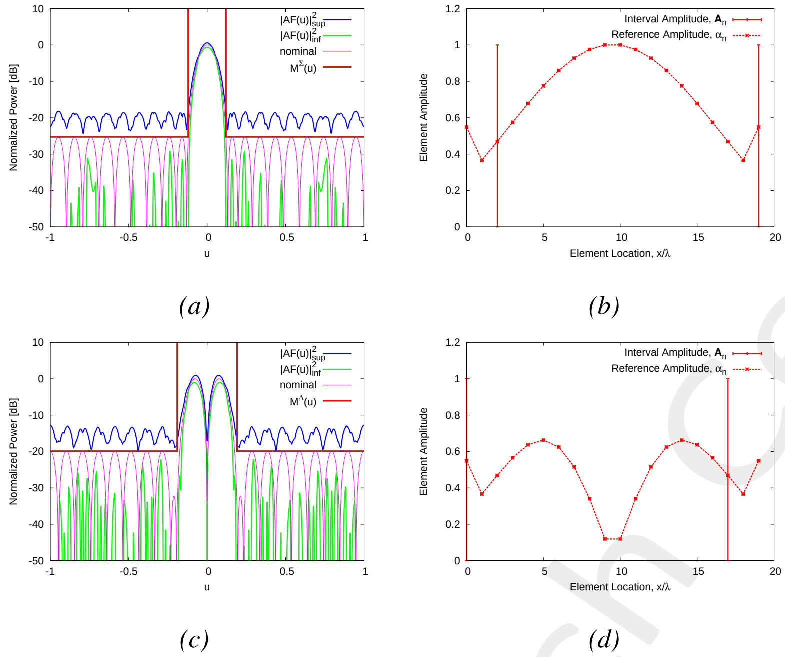

Figure 31. Radiation patterns *(a)(c)* and amplitudes *(b)(d)* for the worst sum beam *(a)(b)* and difference beam *(c)(d)* in terms of BW, considering $F = 2$.

- $P = 8$

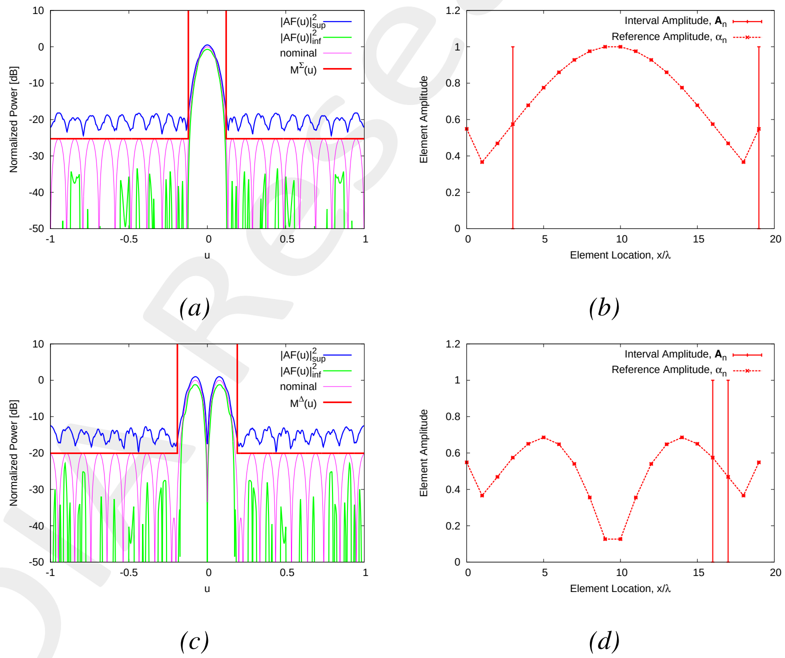

Figure 32. Radiation patterns *(a)(c)* and amplitudes *(b)(d)* for the worst sum beam *(a)(b)* and difference beam *(c)(d)* in terms of BW, considering $F = 2$.

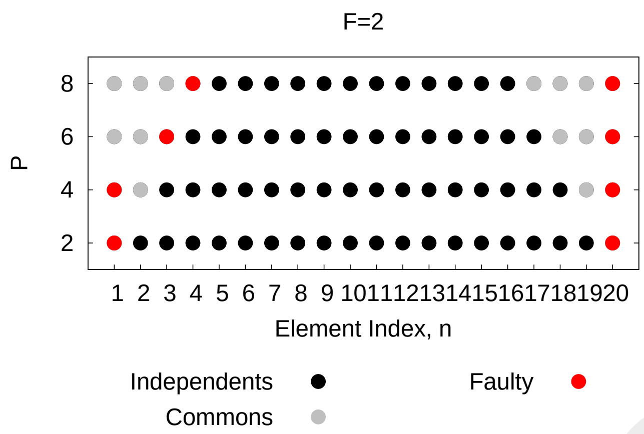

Figure 33. Worst case configurations in terms of BW computed on the Σ beam, and $F = 1$.

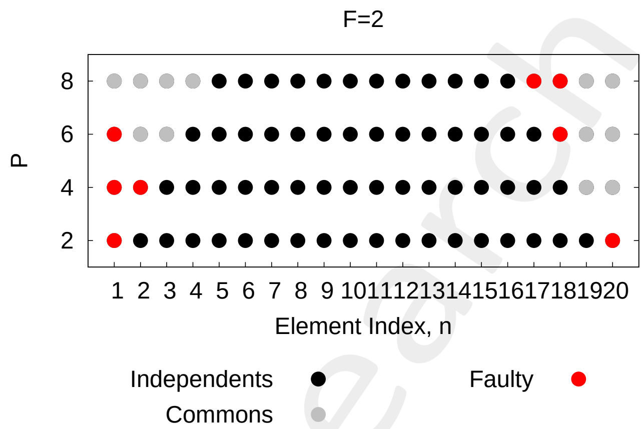

Figure 34. Worst case configurations in terms of BW computed on the Δ beam, and $F = 2$.

More information on the topics of this document can be found in the following list of references.

References

[1] G. Ding, N. Anselmi, W. Xu, P. Li, and P. Rocca, "Interval-bounded optimal power pattern synthesis of array antenna excitations robust to mutual coupling," *IEEE Antennas Wireless Propag. Lett.*, vol. 22, no. 11, pp. 2725-2729, Nov. 2023 (DOI: 10.1109/LAWP.2023.3291428).

[2] N. Anselmi, P. Rocca, and A. Massa, "Tolerance analysis of reconfigurable monopulse linear antenna arrays through interval arithmetic," *J. Electromagn. Waves Appl. J*, pp. 1066-1081, 2023 (DOI: 10.1080/09205071.2023.2224080).

[3] P. Rocca, N. Anselmi, A. Benoni, and A. Massa, "Probabilistic interval analysis for the analytic prediction of the pattern tolerance distribution in linear phased arrays with random excitation errors," *IEEE Trans. Antennas Propag.*, vol. 68, no. 2, pp. 7866-7878, Dec. 2020 (DOI: 10.1109/TAP.2020.2998924).

[4] L. Tenuti, N. Anselmi, P. Rocca, M. Salucci, and A. Massa, "Minkowski sum method for planar arrays sensitivity analysis with uncertain-but-bounded excitation tolerances" *IEEE Trans. Antennas Propag.*, vol. 65, no. 1, pp. 167-177, Jan. 2017 (DOI: 10.1109/TAP.2016.2627548).

[5] N. Anselmi, P. Rocca, M. Salucci, and A. Massa, "Optimization of excitation tolerances for robust beamforming in linear arrays," *IET Microwaves, Antennas & Propagation*, vol. 10, no. 2, pp. 208-214, 2016 (DOI: 10.1049/iet-map.2015.0508).

[6] N. Anselmi, P. Rocca, M. Salucci, and A. Massa, "Power pattern sensitivity to calibration errors and mutual coupling in linear arrays through circular interval arithmetics," *Sensors*, vol. 16, no. 6 (791), pp. 1-14, 2016 (DOI: 10.3390/s16060791).

[7] L. Poli, P. Rocca, N. Anselmi, and A. Massa, "Dealing with uncertainties on phase weighting of linear antenna arrays by means of interval-based tolerance analysis," *IEEE Trans. Antennas Propag.*, vol. 63, no. 7, pp. 3299-3234, Jul. 2015 (DOI: 10.1109/TAP.2015.2421952).

[8] P. Rocca, N. Anselmi, and A. Massa, "Optimal synthesis of robust array configurations exploiting interval analysis and convex optimization," *IEEE Trans. Antennas Propag.*, vol. 62, no. 7, pp. 3603-3612, July 2014 (DOI: 10.1109/TAP.2014.2318071).

[9] T. Moriyama, L. Poli, N. Anselmi, M. Salucci, and P. Rocca, "Real array pattern tolerances from amplitude excitation errors," *IEICE Electronics Express*, vol. 11, no. 17, pp. 1-8, Sep. 2014 (DOI: 10.1587/elex.11.20140571).

[10] N. Anselmi, L. Manica, P. Rocca, and A. Massa, "Tolerance analysis of antenna arrays through interval arithmetic," *IEEE Trans. Antennas Propag.*, vol. 61, no. 11, pp. 5496-5507, Nov. 2013 (DOI: 10.1109/TAP.2013.2276927).

[11] L. Manica, N. Anselmi, P. Rocca, and A. Massa, "Robust mask-constrained linear array synthesis through an interval-based particle swarm optimisation," *IET Microwaves, Antennas and Propagation*, vol. 7, no. 12, pp. 976-984, Sep. 2013 (DOI: 10.1049/iet-map.2013.0203).

[12] P. Rocca, L. Manica, N. Anselmi, and A. Massa, "Analysis of the pattern tolerances in linear arrays with arbitrary amplitude errors," *IEEE Antennas Wireless Propag. Lett.*, vol. 12, pp. 639-642, 2013 (DOI: 10.1109/LAWP.2013.2261912).

[13] L. Manica, P. Rocca, N. Anselmi, and A. Massa, "On the synthesis of reliable linear arrays through interval arithmetic," *IEEE International Symposium on Antennas Propag. (APS/URSI 2013)*, *Orlando, Florida*, *USA*, Jul. 7-12, 2013 (DOI: 10.1109/APS.2013.6710809).

[14] L. Manica, P. Rocca, G. Oliveri, and A. Massa, "Designing radiating systems through interval analysis tools," *IEEE International Symposium on Antennas Propag. (APS/URSI 2013), Orlando, Florida, USA*, Jul. 7-12, 2013 (DOI: 10.1109/APS.2013.6711391).

[15] M. Carlin, N. Anselmi, L. Manica, P. Rocca, and A. Massa, "Exploiting interval arithmetic for predicting real arrays performances - The linear case," *IEEE International Symposium on Antennas Propag. (APS/URSI 2013), Orlando, Florida, USA*, Jul. 7-12, 2013 (DOI: 10.1109/APS.2013.6710810).

[16] N. Anselmi, M. Salucci, P. Rocca, and A. Massa, "Generalised interval-based analysis tool for pattern distortions in reflector antennas with bump-like surface deformations," *IET Microwaves, Antennas & Propagation*, vol. 10, no. 9, p. 909-916, June 2016 (DOI: 10.1049/iet-map.2015.0583).

[17] P. Rocca, L. Poli, N. Anselmi, M. Salucci, and A. Massa, "Predicting antenna pattern degradations in microstrip reflectarrays through interval arithmetic," *IET Microwaves, Antennas & Propagation*, vol. 10, no. 8, pp. 817-826, May 2016 (DOI: 10.1049/iet-map.2015.0837).

[18] P. Rocca, L. Manica, and A. Massa, "Interval-based analysis of pattern distortions in reflector antennas with bump-like surface deformations," *IET Microwaves, Antennas and Propagation*, vol. 8, no. 15, pp. 1277-1285, Dec. 2014 (DOI: 10.1049/iet-map.2014.0162).

[19] P. Rocca, N. Anselmi, and A. Massa, "Interval Arithmetic for pattern tolerance analysis of parabolic reflectors," *IEEE Trans. Antennas Propag.*, vol. 62, no. 10, pp. 4952-4960, Oct. 2014 (DOI: 10.1109/TAP.2014.2342758).